Kirchhoff inversion for incident waves synthesized from common-shot data gathers

Norman Bleistein
Center for Wave Phenomena, Department of Geophysics, Colorado School of Mines, Golden, CO 80401-1887 USA

ABSTRACT
Synthesis is a process for producing reflection responses from more general sources or from prescribed incident waves by combining common-shot data gathers. Synthesis can provide survey-wide data sets, similar in that regard to common-offset data gathers, but with the added advantage that each synthesized data set is a solution to a single wave equation. A common-offset data set does not have this last feature. Thus, synthesized data sets can be processed by true amplitude wave equation migration. The output is then known to be true amplitude, as well, in the same sense as is the output of Kirchhoff inversion. Alternatively, the Kirchhoff inversion of synthesized data has a Beylkin determinant that is expressed in terms of the WKBJ Green's function amplitude. This is in contrast to 3D common offset inversion where the Beylkin determinant is most difficult to compute. We present here a theory of data synthesis based on application of Green's theorem to the ensemble of common-shot gathers and prescribed more general sources or prescribed incident waves. Specific examples include delayed-shot line sources and incident dipping plane waves at the upper surface. We also discuss two cases in which waves are prescribed at depth, back-projected to the upper surface and then used to generate a synthesized data set.

Key words: Kirchhoff inversion, true amplitude wave equation migration, Gaussian beams, ray theory, common-shot data, source synthesis, incident wave synthesis, Green's function, Green's theorem, controlled illumination

1 INTRODUCTION

The paper, Zhang et al [2005] proposes a method of synthesizing data for a delayed-shot line source from the ensemble of common-shot data sets. The paper also suggests synthesis of data in response to incident plane waves. A significant advantage of these synthesized incident waves is that they and their responses can cover the entire range of a survey, in contrast to the individual shot gathers whose surface range is limited by the receiver coverage of each experiment. The possible artifacts arising from the limited range of the shot gathers have not yet been studied for these synthesized migration/inversions. However, we expect that reflection events interior to the range of the shot-gathered data will be imaged in one or more of the synthesized migration/inversion outputs.

Kirchhoff inversion of common-shot data has a simple Beylkin determinant. In fact, the Beylkin determinant is expressible in terms of the amplitude of the upward propagating WKBJ Green's function from the image point to the receiver. This is in contrast to 3D common offset inversion where the Beylkin determinant is most difficult to compute. The key to this difference in computational difficulty of the Beylkin determinants would seem to be that the common-shot data set is a solution of a single wave equation, whereas the common-offset data set is not; each source/receiver pair is a solution of a *different* wave equation.

The synthesis process that we describe here produces a data set that is again the solution of a single wave equation; that is, the synthesized recorded data is the solution to the problem whose incident downward propagating wave is the synthesized incident wave or the response to the synthesized source. We will refer to

this synthesized data set as common-source data even when the synthesizing mechanism starts from a prescribed incident wave rather than a prescribed source. Thus, common-source data is again a solution of the wave equation. The Kirchhoff inversion of such data is derived along the same lines as for common-shot data and leads to a comparably simple Beylkin determinant. The two specific examples mentioned above exhibit this.

The fact that the synthesized common-source data is a solution of the wave equation allows us to apply true-amplitude wave equation migration (WEM) to achieve our modeling and inversion goals; the example of Zhang et al [2005] demonstrates this. Indeed, we use the WEM imaging condition even when using Kirchhoff representations for the propagation of surface data to depth. We know that the asymptotic output of this imaging condition is true-amplitude in the same sense as what we derive from Kirchhoff inversion with WKBJ Green's functions.

Y. Zhang (personal communication) suggested that there is an underlying principle behind these two examples that might yield other practical applications. S. H. Gray observed that this notion had been previously demonstrated in Wapenaar et al [1989], Rietveld et al [1992] and Rietveld [1995], with the latter two references using the discrete matrix approach to modeling and inversion. The purpose of this note is to provide a more classic continuum approach to synthesis by using Green's theorem to synthesize the wave fields. In this regard, this paper has much in common with Wapenaar's, although our point of view and objectives are different. We also provide explicit inversion formulas in terms of general Green's functions, allowing the user to choose exact Green's functions or asymptotic Green's functions at various levels of accuracy: ray theoretic, Gaussian beam, true-amplitude one-way wave equation, for example.

To understand the generalization of the synthesis process, it is important to recognize that the point source experiment generates a Green's function scaled by a source signature. We separate the downward and the upward going waves, with the latter, the acquired record at the receivers, also being a part of that same Green's function. Then, in order to synthesize any other incident source or incident wave and the reflection response to either, we need only intelligently apply Green's theorem, using the ensemble of common-shot sources and their upward propagating reflection responses as the Green's functions in the Green's identity.

In the synthesis of incident plane wave data, we use boundary data in Green's theorem to generate the plane wave and its response from common-shot data, but we could have used an appropriate source at the upper surface. For the delay-shot line, we model the incident wave as a line source, but we could have used appropriate boundary data. It is really a matter of using whichever is more "natural" for the modeling process. For the true amplitude one-way wave equation, we prefer the boundary value form of generating synthesized incident waves. However, as demonstrated in Zhang et al [2003], transforming a source into boundary data in heterogeneous media can involve a pseudo-differential operator, so it is not a straightforward computational procedure.

In the next section, we introduce notation for the propagating waves and their determination via ray theory. While our approach uses general Green's functions, specializing to ray-theoretic and other leading order asymptotic approximations provides insight into the processing mechanisms of the more general expressions that we derive.

In this next section, we also state the general Green's theorem that we will specialize for our two synthesizing methods. Thereafter, we derive the basic synthesis theory and show how the delayed-shot line source synthesis and incident plane wave synthesis conform to that theory. In a heterogeneous medium with the wavespeed depending on the transverse variables at the fixed depth, we can only prescribe a constant traveltime. Consequently, the traveltime gradient is restricted to be vertical at this depth. On the other hand, if the wavespeed is constant on this plane, such as in a homogeneous medium or a depth-dependent medium, we are free to prescribe any incident direction at the fixed depth. That is we introduce a constant unit vector $\hat{\boldsymbol{p}}$; then set $\boldsymbol{p} = \hat{\boldsymbol{p}}/\mathrm{v}(z = H)$, with $\boldsymbol{p}$ being the gradient of the traveltime and v being the wavespeed. For any medium, we set the amplitude of this wave equal to one at $z = H$. We then upward-propagate this wave to the acquisition surface at depth zero. Next, we use this wave at the acquisition surface and the point source responses (common-shot gathers) to synthesize the reflection response to the plane wave at depth. Thereafter, we can downward continue this response function to depth H and apply the true amplitude imaging condition. The computation involved in this application is comparable to the computation for a wave synthesized from a prescribed wave at depth zero. We have only replaced the downward propagation of an incident wave at $z = 0$ with the upward propagation of the incident wave at $z = H$; all other computations are the same in either case. This is an important application of Rietveld's [1995] thesis and Rietveld et al [1992]. Thus, under the name of "Controlled Illumination" these authors have already carried out this particular wave synthesis. The synthesis of a wave at oblique incidence at depth in the more restricted medium is a new result.

Wapenaar et al [1989] discuss the amplitude errors that arise from a non-planar acquisition surface. Difficulty arises in the method because the Green's function or its normal derivative needs to be zero at the acquisition surface in order to carry out an accurate synthesis. For a flat acquisition surface, we can easily express this Green's function in terms of the free-space

Green's function by using the method of images. For the curved surface, the prescribed Green's function is much more difficult to compute. Wapenaar uses the flat surface Green's function for the curved acquisition surface; hence the need for an error analysis. The errors would seem to be not too severe under reasonable assumptions about the background medium. In this paper, we assume a flat acquisition surface throughout.

Finally, we show the commutativity of the operations of synthesis and modeling. On the one hand, we lose the efficiency of inversion over the entire range of a survey from common-source data by reversing the order of operations: in the commuted order, we need to compute all of the common-shot inversions first. On the other hand, examination of the common-shot inversion output in a target zone could lead to a smaller, more efficiently chosen suite of synthesized common-source inversions. For example, if the individual common-shot inversions indicate a limited range of dip directions at the target, synthesized inversions for only that range of dip directions would be necessary to obtain a complete inversion of the data in that region.

A numerical implementation of plane wave synthesis is provided in W. Zhang [2004]. Synthesis with directional plane wave patches is discussed in Xie and Wu [2004], among other papers from Wu and colleagues.

Although we specialize our discussion to ray-theoretic Green's functions in some instances, the synthesis formulas and modeling formulas are all expressed in terms of exact Green's functions, as is the imaging condition. These formulas therefore allow for approximate Green's functions of better quality than the ray-theoretic ones, presumably leading to better quality imaging. Such better quality Green's functions can even be employed in the Kirchhoff inversion formula; see Bleistein et al [2005].

2 MODELING AND NOTATION

A common shot experiment consists of a downgoing wave and its reflection response from the Earth's interior, with that reflection response recorded at the upper surface. As noted earlier, this wave is a band-limited Green's function. We will neglect the source signature for this discussion; it will automatically arise in the processing of field data, since the upward scattered response will be band-limited. Here, it would only appear as a scale factor, $F(\omega)$, in the equations describing the wave fields. In this section we introduce the Green's function that characterizes the common-shot experiment. We will further write down the governing equations for the ray-theoretic approximation of the downgoing part of this Green's function. Thereafter, we introduce a general form of Green's theorem, with both a source term and a boundary value term. It is this representation that we will specialize in the following section to generate our synthesized incident waves and the upward propagating responses to those waves.

2.1 Defining the common-shot experiment

We introduce the notation $G_{\text{FS}}(\boldsymbol{x}, \boldsymbol{x}_s, \omega)$ for the Green's function that models the common-shot experiment. Here

$$\boldsymbol{x}_s = (x_{s1}, x_{s2}, 0), \quad \text{and later} \quad \boldsymbol{x}_r = (x_{r1}, x_{r2}, 0),$$

are the source and receiver coordinates, respectively. The subscript "FS" connotes "free-space." For this Green's function, the medium is assumed to be of infinite extent in all three dimensions. Thus, G_{FS} must satisfy the Helmholtz equation (wave equation in the space-frequency domain) with 3D delta function source and Sommerfeld radiation conditions at infinity, as follows.

$$\begin{aligned}
&\left[\nabla^2 + \frac{\omega^2}{\text{v}^2(\boldsymbol{x})}\right] G_{\text{FS}}(\boldsymbol{x}, \boldsymbol{x}_s, \omega) = -\delta(\boldsymbol{x} - \boldsymbol{x}_s), \\
&\nabla = \left(\frac{\partial}{\partial x_1}, \frac{\partial}{\partial x_2}, \frac{\partial}{\partial x_3}\right), \quad \nabla^2 = \nabla \cdot \nabla, \\
&r G_{\text{FS}} \text{ bounded}, \ r \to \infty, \ r = |\boldsymbol{x}|, \\
&r\left[\frac{\partial G_{\text{FS}}}{\partial r} - \frac{i\omega}{\text{v}(\boldsymbol{x})} G_{\text{FS}}\right] \to 0, \ r \to \infty.
\end{aligned} \tag{1}$$

The choice of sign in the second Sommerfeld condition here is consistent with choosing phase $+i\omega t$ in the forward temporal Fourier transform and $-i\omega t$ in the inverse Fourier transform. This Green's function is called "outgoing." There is a rigorous justification for the nomenclature: when one examines the *energy flux* through a spherical surface of large enough radius, it can be shown that it is pointed outward from that surface, so that the total energy in the interior volume is decreasing with increasing time. (See Bleistein [1984].) Of course, we use the outgoing Green's function to describe more general outgoing waves that satisfy the same radiation conditions.

Mathematically, we also have occasion to make use of the *incoming* Green's functions to represent incoming waves. (The upward propagating reflection response may be thought of as a wave incoming from z "very large", for example.) We obtain the incoming Green's function by just taking the complex conjugate in equation (1); that is,

$$\begin{aligned}
&\left[\nabla^2 + \frac{\omega^2}{\text{v}^2(\boldsymbol{x})}\right] \overline{G_{\text{FS}}(\boldsymbol{x}, \boldsymbol{x}_s, \omega)} = -\delta(\boldsymbol{x} - \boldsymbol{x}_s), \\
&r\overline{G}_{\text{FS}} \text{ bounded}, \ r \to \infty, \\
&r\left[\frac{\partial \overline{G}_{\text{FS}}}{\partial r} + \frac{i\omega}{\text{v}(\boldsymbol{x})} \overline{G}_{\text{FS}}\right] \to 0, \ r \to \infty,
\end{aligned} \tag{2}$$

with $\overline{\cdots}$ denoting complex conjugate. The Green's function $G_{\rm FS}$ is a causal function back in the time domain; that is, this Green's function starts at a finite time and propagates with increasing time. In contrast, $\overline{G}_{\rm FS}$ leads to an *anti-causal* function that propagates from time minus infinity and "turns off" at a finite time.

We propose to identify the downward propagating part of the Green's function $G_{\rm FS}$ of equation (1) with the notation $G_{\rm D}(\boldsymbol{x},\boldsymbol{x}_s,\omega)$. The upward propagating reflection response to this downgoing wave will be denoted by $G_{\rm R}(\boldsymbol{x},\boldsymbol{x}_s,\omega)$. This represents the data observed at the upper surface. Thus,

$$G_{\rm FS}(\boldsymbol{x},\boldsymbol{x}_s,\omega) = G_{\rm D}(\boldsymbol{x},\boldsymbol{x}_s,\omega) + G_{\rm R}(\boldsymbol{x},\boldsymbol{x}_s,\omega). \tag{3}$$

2.2 Ray theory for the downgoing part of the Green's function

Here, we introduce the ray-theoretic determination of $G_{\rm D}(\boldsymbol{x},\boldsymbol{x}_s,\omega)$ as

$$G_{\rm D}(\boldsymbol{x},\boldsymbol{x}_s,\omega) \sim A(\boldsymbol{x},\boldsymbol{x}_s)\exp\{i\omega\tau(\boldsymbol{x},\boldsymbol{x}_s)\}. \tag{4}$$

The travel time τ and the amplitude A in the representation in (4) satisfy the eikonal and transport equations, respectively,

$$[\nabla\tau]^2 = \frac{1}{{\rm v}^2(\boldsymbol{x})}, \quad 2\nabla\tau\cdot\nabla A + A\nabla^2\tau = 0. \tag{5}$$

We solve the eikonal equation by the method of characteristics. The characteristic curves are the rays of *ray theory*:

$$\begin{aligned}
&\frac{d\boldsymbol{x}}{dt} = {\rm v}^2(\boldsymbol{x})\boldsymbol{p}, \quad \boldsymbol{x}\Big|_{t=0} = \boldsymbol{x}_s = (x_{s1}, x_{s2}, 0),\\
&\frac{d\boldsymbol{p}}{dt} = -\frac{\nabla{\rm v}(\boldsymbol{x})}{{\rm v}(\boldsymbol{x})},\\
&\boldsymbol{p}\Big|_{t=0} = \left(p_{I1}, p_{I2}, \sqrt{1/{\rm v}^2(\boldsymbol{x}_s) - p_{I1}^2 - p_{I2}^2}\right),\\
&\frac{d\tau}{dt} = 1, \quad \tau\Big|_{t=0} = 0.
\end{aligned} \tag{6}$$

The first two vector differential equations here are the ray equations and the third differential equation tells us that the running parameter along the rays is the travel time, itself. (This is not the only choice of running parameter along the rays.) The initial ray directions are defined by their initial directions for each fixed $\boldsymbol{x}_s$. This direction is characterized here by the initial values of the first two components of $\boldsymbol{p}$, namely, p_{I1} and p_{I2}, with p_{I3} determined by the eikonal equation as noted in the initial data for $\boldsymbol{p}$ in the second of the ray equations directly above.

The amplitude along the rays is the solution of the transport equation in (5), given by

$$A(\boldsymbol{x},\boldsymbol{x}_s) = \frac{1}{4\pi}\frac{{\rm v}(\boldsymbol{x})}{\sqrt{p_{I3}|J(\boldsymbol{x},\boldsymbol{x}_s)|}}, \tag{7}$$

with

$$J(\boldsymbol{x},\boldsymbol{x}_s) = \frac{\partial(\boldsymbol{x})}{\partial(p_{I1},p_{I2},t)}. \tag{8}$$

This amplitude can also be expressed in terms of the polar angles of $\boldsymbol{p}_I$. We set

$$\begin{aligned}
&\boldsymbol{p}_I = \frac{1}{{\rm v}(\boldsymbol{x}_s)}\hat{\boldsymbol{p}}_I\\
&\hat{\boldsymbol{p}}_I = (\sin\alpha_{I1}\cos\alpha_{I2}, \sin\alpha_{I1}\sin\alpha_{I2}, \cos\alpha_{I1}),
\end{aligned} \tag{9}$$

and then

$$\begin{aligned}
\frac{\partial(\boldsymbol{x})}{\partial(p_{I1},p_{I2},t)} &= \frac{\partial(\boldsymbol{x})}{\partial(\alpha_{I1},\alpha_{I2},t)}\cdot\frac{\partial(\alpha_{I1},\alpha_{I2})}{\partial(p_{I1},p_{I2})}\\
&= \frac{\partial(\boldsymbol{x})}{\partial(\alpha_{I1},\alpha_{I2},t)}\cdot\frac{{\rm v}(\boldsymbol{x}_s)}{p_{I3}\sin\alpha_{I1}}.
\end{aligned} \tag{10}$$

Thus,

$$A(\boldsymbol{x},\boldsymbol{x}_s) = \frac{{\rm v}(\boldsymbol{x})}{4\pi}\sqrt{\frac{\sin\alpha_{I1}}{{\rm v}(\boldsymbol{x}_s)\left|\dfrac{\partial(\boldsymbol{x})}{\partial(\alpha_{I1},\alpha_{I2},t)}\right|}}. \tag{11}$$

Throughout this discussion, we have neglected phase shifts at caustics. For those, we need to introduce an additional phase shift in the amplitude, $iK\pi/2$, with K, the KMAH index, being a count of the number of caustis through which the ray passes on the trajectory from $\boldsymbol{x}_s$ to $\boldsymbol{x}$.

2.3 Green's Theorem and its Consequences

Let us consider any solution of the wave equation in frequency domain and denote it by $u(\boldsymbol{x},\omega)$, again with downgoing and upgoing parts denoted by $u_{\rm D}(\boldsymbol{x},\omega)$ and $u_{\rm R}(\boldsymbol{x},\omega)$, so that

$$u(\boldsymbol{x},\omega) = u_{\rm D}(\boldsymbol{x},\omega) + u_{\rm R}(\boldsymbol{x},\omega). \tag{12}$$

These functions all satisfy the Sommerfeld radiation conditions of equation (1). For $u_{\rm D}$, the radiation condition is satisfied in the lower half-space by virtue of the wave decaying to zero even more rapidly than the Sommerfeld conditions imply. The reason is that this field is generated at depth only so long as there are reflectors or a wave speed that will turn downgoing waves into upgoing waves. Since we have only finite data, we can model the wave speed so that at sufficient depth, neither of these possibilities apply and $u_{\rm D}$ is zero or, at worst, exponentially small in x_3. Physically, where $u_{\rm D}$ is nonzero, we can think of it as an *incoming* wave from infinitiy in x_3.

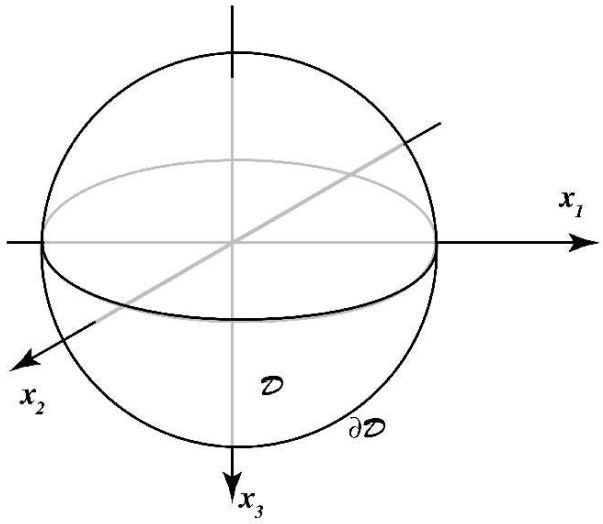

Figure 1. The domain of integration for application of Green's theorem. $\mathcal{D}$ is a spherical volume in 3D and $\partial\mathcal{D}$ is its bounding surface.

We will apply Green's theorem in one of two domains depending on the mechanism by which we generate u. When we use a source on the acquisition surface, we will apply Green's theorem to infinite space as we did in defining G_{FS}, in which case the Green's function will, indeed be just G_{FS}, modulo a source signature that we neglect in this discussion. When we generate u through a downward going wave whose values are given on $x_3 = z = 0$, then we apply Green's theorem on the half-space, $x_3 = z \geq 0$. For the moment then, we will use the "generic" notation $G(\boldsymbol{x}, \boldsymbol{x}'\omega)$ for the Green's function and denote the domain of integration by $\mathcal{D}$.

We state Green's theorem as follows.[1]

$$\begin{aligned} u(\boldsymbol{x},\omega) \quad &= \int_{\mathcal{D}} f(\boldsymbol{x}',\omega) G(\boldsymbol{x},\boldsymbol{x}',\omega) dV' \\ &\quad - \int_{\partial\mathcal{D}} \left[u(\boldsymbol{x}',\omega) \frac{\partial G(\boldsymbol{x},\boldsymbol{x}',\omega)}{\partial n'} \right. \\ &\quad \left. - G(\boldsymbol{x},\boldsymbol{x}',\omega) \frac{\partial u(\boldsymbol{x}',\omega)}{\partial n'} \right] dS'. \end{aligned} \tag{13}$$

In this equation,

(i) $f(\boldsymbol{x}',\omega)$ is a source;
(ii) $\partial\mathcal{D}$ is the boundary of the domain $\mathcal{D}$;
(iii) $\partial n'$ denotes the outward normal derivative on $\partial\mathcal{D}$;
(iv) dV' is the differential volume element of the variable $\boldsymbol{x}'$ over which we integrate in $\mathcal{D}$;
(v) dS' is the differential surface element in $\boldsymbol{x}'$ over which we integrate on the boundary $\partial\mathcal{D}$ of $\mathcal{D}$.

For the mathematically idealized models, $\mathcal{D}$ will either be a sphere as in Figure 1 or it will be a hemisphere with $x_3 > 0$ and disc on $x_3 = 0$ as in Figure 3. In either case, the theory will require that the radius of the sphere approach infinity. Because the range of the observed data is finite, the mathematical theory interprets the missing data as zero data. The consequence of this is the familiar upward facing "diffraction smiles" after inversion, produced by the finite truncation of all integrals. This is the theory's way of interpreting zero data: the inversion creates reflectors that would arise from data that stop at the boundary points of the available data set.

3 SYNTHESIZED INCIDENT AND REFLECTED WAVES

We now have the machinery in place to synthesize other source mechanisms on the upper surface and thereby to define the reflection response to them, as well. Ultimately, the representations will all be expressed in terms of the Green's function $G_{\text{FS}}(\boldsymbol{x}, \boldsymbol{x}_s, \omega)$ of equation (3) and its downward and upward parts denoted by $G_{\text{D}}(\boldsymbol{x}, \boldsymbol{x}_s, \omega)$ and $G_{\text{R}}(\boldsymbol{x}, \boldsymbol{x}_s, \omega)$, respectively. However, we will begin by using the generic Green's function of equation (13).

3.1 Synthesis through a defined source function

Here, we consider the Green's identity of equation (13) with $\mathcal{D}$ being the sphere of radius r depicted in Figure 1. We consider first the surface integral in equation (13) over the boundary $\partial\mathcal{D}$. On that surface, $\partial/\partial n' = \partial/\partial r'$ so that we can rewrite the surface integral as

$$\begin{aligned} I_{\text{surface}} &= \int_{\partial\mathcal{D}} \left[u(\boldsymbol{x}',\omega) \frac{\partial G(\boldsymbol{x},\boldsymbol{x}',\omega)}{\partial r'} \right. \\ &\quad \left. - G(\boldsymbol{x},\boldsymbol{x}',\omega) \frac{\partial u(\boldsymbol{x}',\omega)}{\partial r'} \right] dS' \\ &= \int_{\partial\mathcal{D}} \left[u(\boldsymbol{x}',\omega) \left\{ \frac{\partial}{\partial r'} - \frac{i\omega}{\text{v}(\boldsymbol{x}')} \right\} G(\boldsymbol{x},\boldsymbol{x}',\omega) \right. \\ &\quad \left. - G(\boldsymbol{x},\boldsymbol{x}',\omega) \left\{ \frac{\partial}{\partial r'} - \frac{i\omega}{\text{v}(\boldsymbol{x}')} \right\} u(\boldsymbol{x}',\omega) \right] r'^2 d\Omega' \\ &= \int_{\partial\mathcal{D}} \left[r' u(\boldsymbol{x}',\omega) r' \left\{ \frac{\partial}{\partial r'} - \frac{i\omega}{\text{v}(\boldsymbol{x}')} \right\} G(\boldsymbol{x},\boldsymbol{x}',\omega) \right. \\ &\quad \left. - r' G(\boldsymbol{x},\boldsymbol{x}',\omega) r' \left\{ \frac{\partial}{\partial r'} - \frac{i\omega}{\text{v}(\boldsymbol{x}')} \right\} u(\boldsymbol{x}',\omega) \right] d\Omega' \end{aligned} \tag{14}$$

[1]Note that the wave equation for $u(\boldsymbol{x},\omega)$ has source $-f(\boldsymbol{x}',\omega)$ on the right side of the equation, just as the equation for the Green's function has source $-\delta$.

In the second line of this equation we have done the following.

(i) Replace dS' by $r'^2 d\Omega'$ where $d\Omega'$ is the differential solid angle on the surface of the sphere, $\partial\mathcal{D}$.

(ii) We have added and subtracted the same factor, $i\omega\, u\, G/\mathrm{v}$, to create an operator that mirrors the second of the Sommerfeld radiation conditions in equation (1).

In the third line, we have distributed the multiplier of r' over the separate terms on the integrand. From the Sommerfeld radiation conditions, we know that the factors $r'u$ and $r'G$ remain bounded as $r' \to \infty$. Further, we know that the factors

$$r'\left\{\frac{\partial}{\partial r'} - \frac{i\omega}{\mathrm{v}(\boldsymbol{x}')}\right\} G(\boldsymbol{x}', \boldsymbol{x}, \omega) \quad \text{and}$$

$$r'\left\{\frac{\partial}{\partial r'} - \frac{i\omega}{\mathrm{v}(\boldsymbol{x}')}\right\} u(\boldsymbol{x}', \omega)$$

approach zero as $r' \to \infty$, while the domain of integration in Ω' is bounded, equal in area to 4π. Thus,

$$I_{\text{surface}} \to 0, \quad r' \to \infty. \tag{15}$$

Consequently, in the limit in which the radius of the sphere approaches infinity, only the integral of the source term with the Green's function survives in equation (13). For this synthesis, we will use G_{FS}. That is, for this domain, with the radius allowed to approach infinity

$$u(\boldsymbol{x}, \omega) = \int_{\mathcal{D}} f(\boldsymbol{x}', \omega) G_{\text{FS}}(\boldsymbol{x}, \boldsymbol{x}', \omega) dV'. \tag{16}$$

Here, $\boldsymbol{x}'$ is just a place-holder for $\boldsymbol{x}_s$ and the integration is over the source points for which we have data.

To complete this discussion, we write this last result in terms of the separate downward and upward propagating wave forms comprising G_{FS} in equation (3) thereby defining the downward and upward propagating wave forms of u of equation (12). Thus,

$$\begin{aligned} u_{\text{D}}(\boldsymbol{x}, \omega) &= \int_{\mathcal{D}} f(\boldsymbol{x}', \omega) G_{\text{D}}(\boldsymbol{x}, \boldsymbol{x}', \omega) dV', \\ u_{\text{R}}(\boldsymbol{x}, \omega) &= \int_{\mathcal{D}} f(\boldsymbol{x}', \omega) G_{\text{R}}(\boldsymbol{x}, \boldsymbol{x}', \omega) dV'. \end{aligned} \tag{17}$$

3.1.1 Point source

As a simple test, let us take $f(\boldsymbol{x}', \omega) = \delta(\boldsymbol{x}' - \boldsymbol{x}_s)$. In this case, starting from the integral representation of u in equation (16), we do, indeed, obtain what we should expect, namely,

$$u(\boldsymbol{x}, \boldsymbol{x}_s, \omega) = G_{\text{FS}}(\boldsymbol{x}, \boldsymbol{x}_s, \omega). \tag{18}$$

Here, we have added an extra argument to u to emphasize that it is the response to a point source at $\boldsymbol{x}_s$. Now use equation (17) for the synthesized waves to find that

$$\begin{aligned} u(\boldsymbol{x}_r, \boldsymbol{x}_s, \omega) &= G_{\text{D}}(\boldsymbol{x}, \boldsymbol{x}_s, \omega) + G_{\text{R}}(\boldsymbol{x}, \boldsymbol{x}_s, \omega) \\ &= u_{\text{D}}(\boldsymbol{x}_r, \boldsymbol{x}_s, \omega) + u_{\text{R}}(\boldsymbol{x}, \boldsymbol{x}_s, \omega). \end{aligned} \tag{19}$$

That is, we reproduce the downward and upward components of the common-shot experiment by taking f to be the point source at $\boldsymbol{x}_s$. This is a redundant synthesis that we use only to check that the method of synthesis via a source function *makes sense*. Note that initially both functions are known only at the upper surface and we must compute their values at depth by solving the wave equation.

3.1.2 Delayed-shot line source

Zhang et al [2005] described the wave equation migration of a delayed-shot line and its reflection response. Here, we show how this example fits into the general inversion theory for using sources to generate the synthesized data. To this end, we prescribe the line source of equation (16) as follows:

$$f(\boldsymbol{x}', \omega) = \delta(x_2' - x_{s2})\delta(x_3') \exp\{i\omega p_{01} x_1'\}. \tag{20}$$

The delta functions here restrict the source to a line $x_2' = x_{s2},\ x_3' = 0$, parallel to the x_1 axis and in the acquisition surface; the phase shift represents a linear delay time between shots or, equivalently, a moving point source with speed $1/p_{01}$. We now apply the wave field representation formula of equation (16) to obtain

$$\begin{aligned} u(\boldsymbol{x}, p_{01}, x_{s2}, \omega) &= \int_{\mathcal{D}} G_{\text{FS}}(\boldsymbol{x}, \boldsymbol{x}', \omega) \\ &\qquad \cdot \delta(x_2' - x_{s2})\delta(x_3') \exp\{i\omega p_{01} x_1'\} dV' \\ &= \int_{\mathcal{D}} G_{\text{FS}}(\boldsymbol{x}, x_1', x_{s2}, 0, \omega) \exp\{i\omega p_{01} x_1'\} dx_1' \\ &= u_{\text{D}}(\boldsymbol{x}, p_{01}, x_{s2}, \omega) + u_{\text{R}}(\boldsymbol{x}_r, p_{01}, x_{s2}, \omega). \end{aligned} \tag{21}$$

In this equation,

$$\begin{aligned} u_{\text{D}}(\boldsymbol{x}, p_{01}, x_{s2}, \omega) &= \int_{\mathcal{D}} G_{\text{D}}(\boldsymbol{x}, x_1', x_{s2}, 0, \omega) \\ &\qquad \cdot \exp\{i\omega p_{01} x_1'\} dx_1', \\ u_{\text{R}}(\boldsymbol{x}_r, p_{01}, x_{s2}, \omega) &= \int_{\mathcal{D}} G_{\text{R}}(\boldsymbol{x}, x_1', x_{s2}, 0, \omega) \\ &\qquad \cdot \exp\{i\omega p_{01} x_1'\} dx_1'. \end{aligned} \tag{22}$$

We have changed the arguments of u to reflect the independent variables of this application of the theory. Note that in the first line here we can evaluate the downward

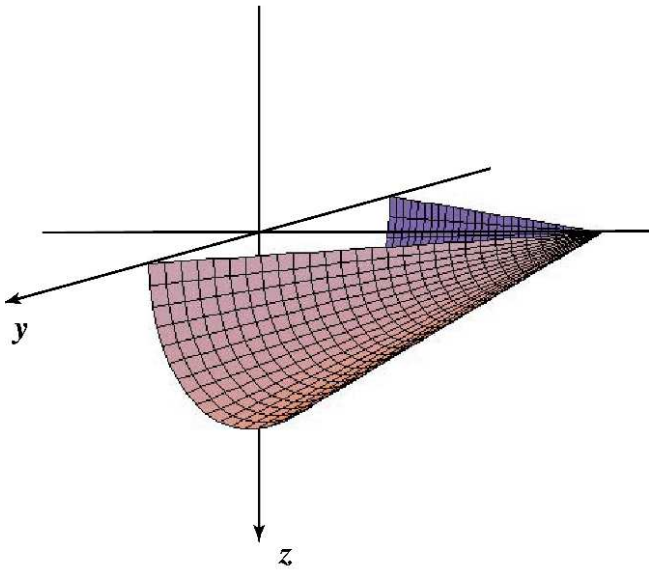

Figure 2. Wave front of the conical wave produced from a delay-shot ensemble of point sources in a homogeneous medium.

propagating wave anywhere in the subsurface because G_{D} is the downward propagating part of the Green's function for the point source. On the other hand, we only know G_{R} at the recording surface and therefore, we can only synthesize the upward propagating wave on that surface. However, these are exactly the two pieces we need to derive an inversion formula for the synthesized data: back-projection of the observed data is a standard component of any inversion technique. We further remark here that the Green's function need not be restricted to a WKBJ approximation, but could be any of the more accurate Green's function representations available in the literature.

3.1.3 u_{D} for homogeneous media

Let us check the theory of the previous section by considering the specialization to homogenous media. That is, we specialize the representation of u_{R} in equation (22) to constant v:

$$u_{\text{D}}(\boldsymbol{x}, p_{01}, x_{s2}, \omega) = \frac{\exp\{i\omega p_{01} x_1\}}{4\pi} \int_{-\infty}^{\infty} \frac{\exp\{i\omega\Phi\}}{|\boldsymbol{x} - (x_1', x_{s2}, 0)|} dx_1', \tag{23}$$

with

$$\Phi = \left|\boldsymbol{x} - (x_1', x_{s2}, 0)\right| / \text{v} + p_{01}(x_1' - x_1). \tag{24}$$

We compute that integral exactly in terms of H_0^1, the Hankel function of the first kind [Erdelyi et al 1953], and then use the known asymptotic expansion of this function to find the asymptotic expansion of u_{D}.

To proceed, we introduce the following changes of variables.

$$y = x_1' - x_1,\ \rho = \sqrt{(x_2 - x_{s2})^2 + x_3^2}, \qquad r = \sqrt{y^2 + \rho^2}. \tag{25}$$

Then the integral representation of u_{D} in equation (23) becomes

$$u_{\text{D}}(\boldsymbol{x}, p_{01}, x_{s2}, \omega) = \exp\{i\omega p_{01} x_1\} \cdot \int_{-\infty}^{\infty} \frac{\exp\{i\omega r/\text{v} + i\omega p_{01} y\}}{4\pi r} dy. \tag{26}$$

The expression under the integral sign here is the Fourier transform in y of the 3D Green's function with transform variable ωp_{01}. Thus, taking account of the phase shift, u_{D} is a solution of the following partial differential equation.

$$\frac{\partial^2 u_{\text{D}}}{\partial x_2^2} + \frac{\partial^2 u_{\text{D}}}{\partial x_3^2} + \frac{\omega^2 q^2}{\text{v}^2} u_{\text{D}} = -\delta(x_2 - x_{s2})\delta(x_3)\exp\{i\omega p_{01} x_1\}, \tag{27}$$

$$q = \sqrt{\frac{1}{\text{v}^2} - p_{01}^2}.$$

We use the known expression for the Green's function in 2D [Bleistein, 1984] to write the solution of this equation as

$$u_{\text{D}}(\boldsymbol{x}, p_{01}, x_{s2}, \omega) = \frac{i\text{sgn}(\omega)}{4} H_0^1(\omega q r/\text{v}) \exp\{i\omega p_{01} x_1\}. \tag{28}$$

and then use the known asymptotic expansion of the Hankel function [Bleistein, 1984] to find that

$$u_{\text{D}}(\boldsymbol{x}, p_{01}, x_{s2}, \omega) \sim \frac{1}{2\sqrt{2|\omega| q r/\text{v}}} \cdot \exp\{i\omega[p_{01} x_1 + q\rho]/\text{v} + i\pi/4\text{sgn}(\omega)\}. \tag{29}$$

We now set

$$\sin\gamma_0 = \text{v} p_{01}, \quad \cos\gamma_0 = \text{v} q, \tag{30}$$

and then rewrite this last representation for u_{D} in equation (28) as

$$u_{\text{D}}(\boldsymbol{x}, p_{01}, x_{s2}, \omega) \sim \frac{1}{2\sqrt{2|\omega| q r/\text{v}}} \cdot \exp\{i\omega[x_1 \sin\gamma_0 + \rho\cos\gamma_0] + i\pi/4\text{sgn}(\omega)\}. \tag{31}$$

In this form, it is easy to see that the wave front forms a "line" in x_1, ρ making a dip angle γ_0 with the x_1 direction. Since ρ is a radial variable in $(x_2 - x_{s2}, x_3)$ we see that the wave front lies on a cone as in Figure 2

3.1.4 Ray theory for $u_{\rm D}$

The asymptotic analysis of the previous section provides us with needed information for generation of $u_{\rm D}$ in a heterogeneous medium. The asymptotic solution (31) provides initial data for the ray-theoretic solution in heterogeneous media. We set

$$u_{\rm D}(\boldsymbol{x}, p_{01}, x_{s2}, \omega) \sim \frac{A_{\rm D}(\boldsymbol{x}, p_{01}, x_{s2})}{\sqrt{|\omega|}} \cdot \exp\{i\omega\tau_{\rm D}(\boldsymbol{x}, p_{01}, x_{s2}) + i\tfrac{\pi}{4}\mathrm{sgn}(\omega)\}. \tag{32}$$

The rays for this solution will emanate from the single line and the amplitude will have singular behavior in the neighborhood of that line. The ray equations and initial data for $\tau_{\rm D}$ and $A_{\rm D}$ are

$$\begin{aligned}
&\frac{d\boldsymbol{x}}{d\sigma} = \boldsymbol{p} = \nabla\tau_{\rm D},\\
&\qquad \boldsymbol{x}\Big|_{\sigma=0} = \boldsymbol{x}_s = (x_{s1}, x_{s2}, 0),\\
&\frac{d\tau_{\rm D}}{d\sigma} = \frac{1}{\mathrm{v}^2(\boldsymbol{x})}, \quad \tau_{\rm D}\Big|_{\sigma=0} = p_{01}x_{s1}, \sigma = 0,\\
&\frac{\boldsymbol{dp}}{d\sigma} = \frac{1}{\mathrm{v}(\boldsymbol{x})}\nabla\left[\frac{1}{\mathrm{v}(\boldsymbol{x})}\right],\\
&\boldsymbol{p}\Big|_{\sigma=0} = \boldsymbol{p}_0 = (p_{01}, q\cos\gamma_1, q\sin\gamma_1), \sigma = 0,\\
&\qquad q = \sqrt{1/\mathrm{v}^2(\boldsymbol{x}_s) - p_{01}^2},\\
&2\nabla\tau_{\rm D}\cdot\nabla A_{\rm D} + A_{\rm D}\nabla^2\tau_{\rm D} = 0,\\
&\qquad A_{\rm D} \sim \frac{1}{2\sqrt{2\pi\rho\, q(\boldsymbol{x}_s)/\mathrm{v}}}, \quad \sigma \to 0.
\end{aligned} \tag{33}$$

For each fixed value of p_{01} and x_{s2}, the rays are functions of $(\sigma, x_{s1}, \gamma_1)$.

Caution!

If v $\neq$ constant on the initial line, then p_{01} = constant does not produce a cone of constant angle, because q is not constant. However, p_{01} = constant does produce a linear delay in shots. For a fixed cone angle, we should set

$$\tau_{\rm D}(x_{s1}, \gamma_0, x_{s2}) = \tau_{\rm D}(x_{s10}, \gamma_0, x_{s2}) + \cos\gamma_0 \int_{x_{s10}}^{x_{s1}} \frac{dx'}{\mathrm{v}(x', x_{s2}, 0)}$$

and then rewrite that solution as

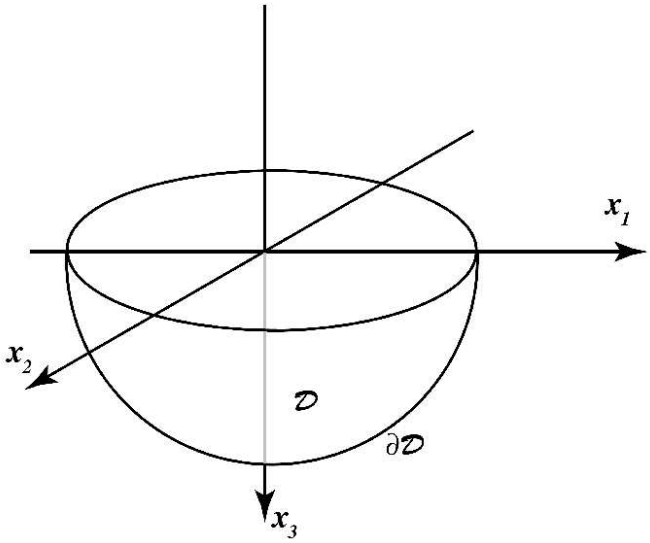

Figure 3. The new domain of integration for application of Green's theorem. $\mathcal{D}$ is a spherical volume in 3D and $\partial\mathcal{D}$ is its bounding surface.

$$u_{\rm D}(\boldsymbol{x}, \gamma_0, x_{s2}, \omega) \sim \frac{A_{\rm D}(\boldsymbol{x}, \gamma_0, x_{s2})}{\sqrt{|\omega|}} \cdot \exp\{i\omega\tau_{\rm D}(\boldsymbol{x}, \gamma_0, x_{s2}) + i\tfrac{\pi}{4}\mathrm{sgn}(\omega)\}$$

This completes our preliminary discussion of the generation of the response to sources synthesized from point source data. We have stated a general result for the synthesis of the down going wave and for the response at the receiver array from point source data in equation (17) and we have presented two examples, the first being a simple check on the formulas to see that the common-shot data set is reproduced by the synthesis process and the second being the example of a delayed-shot line source.

3.2 Synthesis through prescribed boundary data

We return to Green's theorem as stated in equation (13). Now, however, we will take the source term f to be equal to zero and integrate over the hemispherical domain of Figure 3. Thus, we restate equation (13) as

$$u(\boldsymbol{x}, \omega) = -\int_{\partial\mathcal{D}} \left[u(\boldsymbol{x}', \omega)\frac{\partial G(\boldsymbol{x}, \boldsymbol{x}', \omega)}{\partial n'} - G(\boldsymbol{x}, \boldsymbol{x}', \omega)\frac{\partial u(\boldsymbol{x}', \omega)}{\partial n'}\right] dS' \tag{34}$$

Again, we take the limit as the spherical radius approaches infinity. As above, the integral on the hemisphere can be shown to approach zero in that limit by

applying the Sommerfeld radiation conditions given in equation (1). The domain in this last equation then reduces to the acquisition surface where $x_3' = 0$. That is,

$$u(\boldsymbol{x},\omega) = \int\limits_{x_3'=0} \left[u(\boldsymbol{x}',\omega)\frac{\partial G(\boldsymbol{x},\boldsymbol{x}',\omega)}{\partial x_3'} - G(\boldsymbol{x},\boldsymbol{x}',\omega)\frac{\partial u(\boldsymbol{x}',\omega)}{\partial x_3'}\right] dx_1' dx_2'. \tag{35}$$

Here, we have used the fact that $\partial/\partial n' = -\partial/\partial x_3'$ on $x_3' = 0$.

We face two challenges in using this equation to synthesize data. First, we need to express the boundary values of G in terms of the boundary values of G_{FS}. Second, for the latter function, we only know the function values on the acquisition surface, $x_3 = 0$, and we *do not know* the boundary values of its normal derivative. Thus, we cannot simply replace G by G_{FS} as we did above in synthesizing new data by prescribing the source function f. We need to require of G that

$$\frac{\partial G(\boldsymbol{x},\boldsymbol{x}',\omega)}{\partial x_3'} = 0, \quad x_3' = 0. \tag{36}$$

We can express this Green's function in terms of G_{FS} by the method of images after creating the appropriate "thought experiment" under reasonable constraints on the model. We first assume that the wave speed v is constant in the neighborhood of $x_3 = 0+$. Then, we continue the wave speed to $x_3 < 0$ as an even function of x_3, thus creating a mirror image of the positive x_3 domain in the upper half space. That is,

$$\mathrm{v}(\boldsymbol{x}^*) = \mathrm{v}(\boldsymbol{x}), \quad \boldsymbol{x}^* = (x_1, x_2, -x_3). \tag{37}$$

Now set

$$G(\boldsymbol{x},\boldsymbol{x}',\omega) = G_{\text{FS}}(\boldsymbol{x},\boldsymbol{x}',\omega) + G_{\text{FS}}(\boldsymbol{x},\boldsymbol{x}'^*,\omega). \tag{38}$$

For this function, when $x_3' = 0$, the arguments of the two functions on the right side of the equation are equal and

$$G(\boldsymbol{x},\boldsymbol{x}',\omega) = 2G_{\text{FS}}(\boldsymbol{x},\boldsymbol{x}',\omega), \quad x_3' = 0. \tag{39}$$

On the other hand, when we take the x_3' derivative on the right hand side of equation (38), the two terms are of opposite sign and of equal argument when we set x_3' equal to zero. Hence, there sum is equal to zero and G satisfies the imposed boundary condition of equation (36).

Note that the method of images will not work when the acquisition surface is not flat. Wapenaar et al [1989] discuss the errors that occur when we use the approximation in equation (39) anyway.

As a consequence of this thought experiment, we can now rewrite the representation of u in equation (35) as

$$u(\boldsymbol{x},\omega) = -2\int_{x_3'=0} G_{\text{FS}}(\boldsymbol{x},\boldsymbol{x}',\omega) \cdot\frac{\partial u(\boldsymbol{x}',\omega)}{\partial x_3'} dx_1' dx_2'. \tag{40}$$

Again we can decompose this representation into the incident downward propagating synthesized wave and the upward propagating synthesized response by using equation (3) for G_{FS}. That is,

$$u(\boldsymbol{x},\omega) = u_{\text{D}}(\boldsymbol{x},\omega) + u_{\text{R}}(\boldsymbol{x},\omega), \tag{41}$$

with

$$\begin{aligned} u_{\text{D}}(\boldsymbol{x},\omega) &= -2\int_{x_3'=0} G_{\text{D}}(\boldsymbol{x},\boldsymbol{x}',\omega) \cdot\frac{\partial u(\boldsymbol{x}',\omega)}{\partial x_3'} dx_1' dx_2', \\ u_{\text{R}}(\boldsymbol{x}_r,\omega) &= -2\int_{x_3'=0} G_{\text{R}}(\boldsymbol{x}_r,\boldsymbol{x}',\omega) \cdot\frac{\partial u(\boldsymbol{x}',\omega)}{\partial x_3'} dx_1' dx_2'. \end{aligned} \tag{42}$$

Note that in the first line here we can evaluate the downward propagating wave anywhere in the subsurface because G_{D} is the downward propagating part of the Green's function for the point source. On the other hand, we only know G_{R} at the recording surface and therefore we can only synthesize the upward propagating wave on that surface. However, as previously, these are exactly the two pieces we need to derive an inversion formula for the synthesized data.

3.2.1 Downward propagation of $u_{\text{R}}(\boldsymbol{x}_r,\omega)$

Given the data $u_{\text{R}}(\boldsymbol{x}_r,\omega)$ we could now propagate it downward by using a Green's function technique similar to those that we used in earlier sections. However, $u_{\text{R}}(\boldsymbol{x}_r,\omega)$ is a hybrid wave: it is *upward propagating* and does not radiate towards $+\infty$ in x_3; at any depth, it decays in that direction only by virtue of the loss of energy to reflection in the overburden. This leaves us some freedom as to which Green's function we use to project these data back into the Earth. As long as we stay in the lower half-space, we can use either the inward or outward radiating Green's function and still be assured that the integral on a hemisphere of increasing radius will decay to zero in the limit. However, our physical intuition tells us that we want to propagate backwards in time, which is achieved by using the inward propagating Green's function $\overline{G}$ of equation (2). That is, we apply a Green's theorem that is mathematically rigorous and

satisfies our physical intuition about how to downward propagate $u_{\rm R}(\boldsymbol{x}_r,\omega)$.

Alternatively, thinking in terms of the WKBJ form of the wave fields—mainly, the phase of that form that characterizes the traveltime on each wave—helps us decide on how to proceed. The wave field $u_{\rm R}(\boldsymbol{x},\omega)$ has accumulated travel time on its upward propagation. Thus, we want to use a Green's function that would *reduce* the total travel time as the wave is propagated back into the Earth by its Green's function representation. Clearly, that Green's function is $\overline{G}$.

Thus, in analogy with the Green's function representation of equation (35), we now set

$$\begin{aligned} u_{\rm R}(\boldsymbol{x},\omega) = \int_{x_{r3}=0} \Bigg[& u_{\rm R}(\boldsymbol{x}_r,\omega)\frac{\partial\overline{G(\boldsymbol{x},\boldsymbol{x}_r,\omega)}}{\partial x_{r3}} \\ & \cdot -\overline{G(\boldsymbol{x},\boldsymbol{x}_r,\omega)}\frac{\partial u_{\rm R}(\boldsymbol{x}_r,\omega)}{\partial x_{r3}}\Bigg] dx_{r1}dx_{r2}. \end{aligned} \tag{43}$$

We are assured that the integral on the hemisphere approaches zero as the radius approaches infinity by applying the Sommerfeld radiation conditions of the anticausal Green's function in equation (2).

In equation (43) for $u_{\rm R}(\boldsymbol{x},\omega)$, we know $u_{\rm R}(\boldsymbol{x}_r,\omega)$, but we do not know its derivative with respect to x_{r3} at $x_{r3}=0$. Thus, we need a Green's function that satisfies the boundary condition

$$\overline{G(\boldsymbol{x},\boldsymbol{x}_r,\omega)} = 0, \quad x_{r3}=0. \tag{44}$$

By using the same logic that led to the synthesis above, we can show that

$$\overline{G(\boldsymbol{x},\boldsymbol{x}_r,\omega)} = \overline{G_{\rm D}(\boldsymbol{x},\boldsymbol{x}_r,\omega)} - \overline{G_{\rm D}(\boldsymbol{x},\boldsymbol{x}_r^*,\omega)} \tag{45}$$

will do the trick! This sum on the right here is equal to zero at $x_{r3}=0$, while the first derivatives with respect to x_{r3} add to give twice the derivative of the first term when $x_{r3}=0$. Thus, we find that the synthesized data can be downward continued into $x_3>0$ by the formula

$$\begin{aligned} u_{\rm R}(\boldsymbol{x},\omega) = 2\int_{x_{r3}=0} & u_{\rm R}(\boldsymbol{x}_r,\omega) \\ & \cdot\frac{\partial\overline{G_{\rm D}(\boldsymbol{x},\boldsymbol{x}_r,\omega)}}{\partial x_{r3}} dx_{r1}dx_{r2}. \end{aligned} \tag{46}$$

Note that if we set

$$G_{\rm D}(\boldsymbol{x},\boldsymbol{x}_r,\omega) = A(\boldsymbol{x},\boldsymbol{x}_r)\exp\{i\omega\tau(\boldsymbol{x},\boldsymbol{x}_r)\}, \tag{47}$$

this formula becomes more familiar as

$$\begin{aligned} u_{\rm R}(\boldsymbol{x},\omega) &= 2i\omega\int_{x_{r3}=0}\frac{\partial\tau(\boldsymbol{x},\boldsymbol{x}_r)}{\partial\boldsymbol{x}_{r3}}A(\boldsymbol{x},\boldsymbol{x}_r) \\ &\quad\cdot u_{\rm R}(\boldsymbol{x}_r,\omega)\exp\{-i\omega\tau(\boldsymbol{x},\boldsymbol{x}_r)\}dx_{r1}dx_{r2} \\ &= 2i\omega\int_{x_{r3}=0}\frac{\cos\alpha_r}{\mathrm{v}(\boldsymbol{x}_r)}A(\boldsymbol{x},\boldsymbol{x}_r) \\ &\quad\cdot u_{\rm R}(\boldsymbol{x}_r,\omega)\exp\{-i\omega\tau(\boldsymbol{x},\boldsymbol{x}_r)\}dx_{r1}dx_{r2}. \end{aligned} \tag{48}$$

Here, α_r is the angle between the downward normal to the acquisition surface and $\nabla_{x_r}\tau$. However, the form in equation (46) indicates that we could use a Green's function of better quality than is produced by ray theory. Further, we could just solve the wave equation for $u_{\rm R}(\boldsymbol{x},\omega)$ with the prescribed boundary condition as is done in wave equation migration.

Note that the downward propagation of the data $u_{\rm R}(\boldsymbol{x}_r,\omega)$ by equation (46) or equation (48) also applies to data synthesized via a source mechanism as discussed earlier in this section. That is, we use equation (42) to determine the data $u_{\rm R}(\boldsymbol{x}_r,\omega)$ and then use equation (46) or (48) to project these data into the Earth. We postponed the discussion of downward continuation of data generated by a synthesized source until after we had the machinery of the present discussion in place.

3.2.2 Plane wave incidence

Here we demonstrate the application of synthesis of wave fields via boundary values. We consider a plane wave incident from above at $x_3=0$ in a medium that is homogeneous from above through $x_3=0+$. That is, we set

$$\begin{aligned} & u(x_1,x_2,0,\omega) = \exp\{i\omega[p_{01}x_1+p_{02}x_2]\}, \\ & \boldsymbol{p}_0 = (p_{01},p_{02},p_{03}), \quad p_{03}>0, \end{aligned} \tag{49}$$

with $\boldsymbol{p}$ a constant vector.

We substitute this wave form into equation (42) and find that

$$\begin{aligned} u_{\rm D}(\boldsymbol{x},\omega) &= -2i\omega p_{03}\int_{x_3'=0} G_{\rm D}(\boldsymbol{x},\boldsymbol{x}',\omega) \\ &\quad\cdot\exp\{i\omega\boldsymbol{p}_0\cdot\boldsymbol{x}'\}dx_1'dx_2', \\ u_{\rm R}(\boldsymbol{x}_r,\omega) &= -2i\omega p_{03}\int_{x_3'=0} G_{\rm R}(\boldsymbol{x}_r,\boldsymbol{x}',\omega) \\ &\quad\cdot\exp\{i\omega\boldsymbol{p}_0\cdot\boldsymbol{x}'\}dx_1'dx_2'. \end{aligned} \tag{50}$$

We see here that the synthesized wave forms are the 2D Fourier transforms of the elements of the downward and upward propagating components of the 3D point

source Green's function, multiplied by $-2i\omega p_{03}$. In this case, when we carry out inversion, the constant factor of $-2i\omega p_{03}$ would appear in both the numerator and the denominator of the imaging condition and, thus, can be disregarded.

3.2.3 Homogeneous medium

As a check on the method, let us specialize u_{D} to the case of a homogeneous medium; that is, set v = constant. Then,

$$\begin{aligned} u_{\text{D}}(\boldsymbol{x},\omega) &= -2i\omega p_{03}\int_{x_3'=0} dx_1'dx_2' \\ &\cdot\frac{\exp\left\{i\omega\left[\left|\boldsymbol{x}-(x_1',x_2',0)\right|/\text{v}+p_{01}x_1'+p_{02}x_2'\right]\right\}}{4\pi\left|\boldsymbol{x}-(x_1',x_2',0)\right|} \\ &= -2i\omega p_{03}\exp\{i\omega p_{01}x_1+p_{02}x_2\} \\ &\cdot\int_{x_3'=0} dx_1'dx_2'\frac{\exp\left\{i\omega\Phi\right\}}{4\pi\left|\boldsymbol{x}-(x_1',x_2',0)\right|}, \end{aligned} \tag{51}$$

with

$$\begin{aligned} \Phi &= \left|\boldsymbol{x}-(x_1',x_2',0)\right|/\text{v} \\ &\quad +p_{01}(x_1'-x_1)+p_{02}(x_2'-x_2). \end{aligned} \tag{52}$$

The integral in the second line of equation (51) is the 2D Fourier transform of the 3D Green's function. Hence, it is the 1D Green's function which is

$$-\exp\{i\omega p_{03}x_3\}/2i\omega p_{03}.$$

Thus, when we substitute the expression for the integral in the second line of the plane wave representation of $u_{\text{D}}(\boldsymbol{x},\omega)$ in equation (51), we arrive at the plane wave representation of equation (49), but now for $x_3>0$.

3.2.4 Ray theory for plane wave incidence

As in the discussion of the line source, above, we might want to generate $u_{\text{D}}(\boldsymbol{x},\omega)$ by ray theory. The ray equations of the previous example, equation (33) remain unchanged, but the data at the upper surface changes as follows.

$$\begin{aligned} &u_{\text{D}} = A_{\text{D}}\exp\{i\omega\tau_{\text{D}}\}, \\ &\boldsymbol{x}\Big|_{\sigma=0} = \boldsymbol{x}_s = (x_{s1},x_{s2},0), \\ &\boldsymbol{p}\Big|_{\sigma=0} = \boldsymbol{p}_0 = (p_{01},p_{02},p_{03}),\ ||\boldsymbol{p}_0|| = \frac{1}{\text{v}(\boldsymbol{x}_s)}, \\ &\tau_{\text{D}}\Big|_{\sigma=0} = p_{01}x_{s1}+p_{02}x_{s2}, \\ &A_{\text{D}}\Big|_{\sigma=0} = 1. \end{aligned} \tag{53}$$

Given $\boldsymbol{x}$ and $\boldsymbol{p}_0$, we can eliminate $\boldsymbol{x}_s$ through ray tracing, so that the final result is not a function of $\boldsymbol{x}_s$, which plays no role in the synthesized wave form. We use the subscript s here just to indicate that the rays start from the upper surface.

We have now derived a theory for synthesis of incident waves and their reflection response from common-shot data. Further, we demonstrated this method for synthesizing plane wave incidence and its reflection response.

4 INVERSION

At this point, we have derived a method for synthesizing the reflection response to waves generated by sources or defined incident waves. In each case, we showed how the incident wave can be generated from point source data, leading to a synthesis generated from common-shot records. Whether we start the synthesis from an incident wave or a prescribed source, we refer to the synthesized data as common-source data. We do this because the inversion procedure is the same for both types of synthesis and follows along the lines of the inversion of common-shot data.

We can now write down inversion formulas for the reflectivity function $\mathcal{R}(\boldsymbol{x},\theta)$ by starting from the true amplitude imaging condition of wave equation migration, namely,

$$\mathcal{R}(\boldsymbol{x},\theta) = \frac{1}{2\pi}\int\frac{u_{\text{R}}(\boldsymbol{x},\omega)}{u_{\text{D}}(\boldsymbol{x},\omega)}d\omega. \tag{54}$$

Here, we have omitted the extra arguments in u_{D} and u_{R} that characterized a specific wave field synthesis. If we now use the downward propagator of equation (46) to express $u_{\text{R}}(\boldsymbol{x},\omega)$ in terms of $u_{\text{R}}(\boldsymbol{x}_r,\omega)$, then this last result becomes

$$\begin{aligned} \mathcal{R}(\boldsymbol{x},\theta) = \frac{1}{\pi}\int\int_{x_{r3}=0}&\frac{u_{\text{R}}(\boldsymbol{x}_r,\omega)}{u_{\text{D}}(\boldsymbol{x},\omega)} \\ &\cdot\frac{\partial\overline{G_{\text{D}}(\boldsymbol{x},\boldsymbol{x}_r,\omega)}}{\partial x_{r3}}dx_{r1}dx_{r2}d\omega. \end{aligned} \tag{55}$$

In this form, we can still use any quality of Green's function G_{D} and are not restricted to ray-theoretic Green's functions.

4.1 Common-shot inversion derived from equation (55)

As a simple check of this result, we introduce the ray-theoretic Green's function representation of the downward continued wave as in equation (48) and also specialize to the point source as given by equation (4). With

these subsitutions into the last equation, we obtain the familiar common shot inversion formula

$$\mathcal{R}(\boldsymbol{x},\theta) = 2\int \frac{\cos\alpha_r}{\mathrm{v}(\boldsymbol{x}_r)}\frac{A(\boldsymbol{x},\boldsymbol{x}_r)}{A(\boldsymbol{x},\boldsymbol{x}_s)} \cdot D(\boldsymbol{x}_r,\boldsymbol{x}_s,\boldsymbol{x})dx_{r1}dx_{r2}$$
$$D(\boldsymbol{x}_r,\boldsymbol{x}_s,\boldsymbol{x}) = \frac{1}{2\pi}\int d\omega i\omega u_{\mathrm{R}}(\boldsymbol{x}_r,\omega) \cdot \exp\{-i\omega\left[\tau(\boldsymbol{x},\boldsymbol{x}_r)+\tau(\boldsymbol{x},\boldsymbol{x}_s)\right]\}. \tag{56}$$

This is the standard form of common-shot Kirchhoff inversion as found in Keho and Beydoun [1988] and, with minor constant correction, in Hanitzsch [1997]. This result provides the simplest of checks on the general formula of inversion of synthesized waves as expressed by equation (55).

5 PRESCRIBING A WAVE AT DEPTH

Even for a medium that is homogeneous at the upper surface, a plane wave at the upper surface does not remain planar as it propagates into the Earth. At depth, in a heterogeneous medium, we could not even start with a plane wave, unless its gradient is vertical, as we will show, below. There are two ways to deal with this limitation. One is to consider a wave with constant traveltime and constant amplitude at a given depth. This is the example that Rietveld [1995] and Rietveld et al [1992] considered under the name of controlled illumination. For such a wave, the gradient is vertical; that means that the incident wave direction on a reflector intersecting the plane at that depth is fixed at vertical. The other alternative is to consider homogeneous or depth-dependent media. In this case, we can vary the direction of the incident wave and thereby control the incident angle on reflectors intersecting the plane at depth.

We first explain why these constraints are in place and then we examine both types of prescribed waves at depth, first for the fully heterogeneous medium and then for the depth-dependent or homogenous medium.

5.1 Prescribing traveltime at a horizontal plane

We consider here the problem of defining a traveltime on a horizontal plane at depth. It would not be of great value to us to prescribe this traveltime with a gradient that varied in direction from one point to the next; for that, we might as well content ourselves with the synthesis of plane wave data at the upper surface. Therefore, on a plane at a depth, $z = H$, let us introduce the travel time gradient by first introducing a constant unit vector $\hat{\boldsymbol{p}}_{_H}$ and then setting

$$\nabla\tau(\boldsymbol{x}_{_H}) = \boldsymbol{p}_{\mathrm{H}} = \frac{\hat{\boldsymbol{p}}}{\mathrm{v}(\boldsymbol{x}_{_H})}, \quad \boldsymbol{x}_{_H} = (x_1, x_2, H),$$

$$\tau(\boldsymbol{x}_{_H}) = \tau(\boldsymbol{x}_{H0}) + \int_{\boldsymbol{x}_{H0}}^{\boldsymbol{x}_H}\left(\frac{\hat{p}_1}{\mathrm{v}(\boldsymbol{x}'_{_H})}, \frac{\hat{p}_2}{\mathrm{v}(\boldsymbol{x}'_{_H})}\right)\cdot d\boldsymbol{s}, \tag{57}$$
$$d\boldsymbol{s} = (dx'_1, dx'_2).$$

In this last equation, we interpret the integration as being on a curvilinear path connecting the two points, $\boldsymbol{x}_{H0}$ and $\boldsymbol{x}_{_H}$.

The question that arises here is whether or not the function $\tau(\boldsymbol{x}_{_H})$ is single-valued. It is relatively easy to answer. Let is consider two different paths between the endpoints. Then the difference between the values on the two different paths would be the integral on the closed path obtained by combining the two of them; that is,

$$\Delta\tau(\boldsymbol{x}_{_H}) = \oint\left(\frac{\hat{p}_1}{\mathrm{v}(\boldsymbol{x}'_{_H})}, \frac{\hat{p}_2}{\mathrm{v}(\boldsymbol{x}'_{_H})}\right)\cdot d\boldsymbol{s}, \tag{58}$$

Green's theorem tells us that we can rewrite this line integral as an area integral over the interior of the region bounded by the closed path; that is,

$$\begin{aligned}\Delta\tau(\boldsymbol{x}_{_H}) &= \int\left\{\hat{p}_1\frac{\partial}{\partial x'_2}\left[\frac{1}{\mathrm{v}(\boldsymbol{x}'_{_H})}\right] - \hat{p}_2\frac{\partial}{\partial x'_1}\left[\frac{1}{\mathrm{v}(\boldsymbol{x}'_{_H})}\right]\right\}dx'_1dx'_2 \\ &= -\int\left[\frac{1}{\mathrm{v}^2(\boldsymbol{x}'_{_H})}\right]\left\{\hat{p}_1\frac{\partial \mathrm{v}(\boldsymbol{x}'_{_H})}{\partial x'_2} - \hat{p}_2\frac{\partial \mathrm{v}(\boldsymbol{x}'_{_H})}{\partial x'_1}\right\}dx'_1dx'_2.\end{aligned} \tag{59}$$

For single-valuedness of $\tau(\boldsymbol{x}_{_H})$, we need that this area integral always be equal to zero. Thus, we need that the integrand be equal to zero; that is,

$$\hat{p}_1\frac{\partial \mathrm{v}(\boldsymbol{x}'_{_H})}{\partial x'_2} - \hat{p}_2\frac{\partial \mathrm{v}(\boldsymbol{x}'_{_H})}{\partial x'_1}. \tag{60}$$

One way to make this happen is for $\hat{p}_1 = \hat{p}_2 = 0$. This is Reitveld's choice. It leads to illumination at the depth H with vertical incidence of the resulting wave. Another way for this equation to be satisfied is if the two first derivatives of the wavespeed are equal to zero. This is the case for a homogeneous medium or for a depth dependent medium where the two transverse derivatives of the velocity are both zero. Below, we consider setting the two slownesses equal to zero with vertical wave incidence and we consider a unidirectional wave for the depth-dependent or homogeneous medium.

There are also less interesting cases, where, for example, $p_1 = 0$ and $\partial \mathrm{v}/\partial x_1' = 0$. That is, we consider a wave at depth for which the wave speed is a function of (x_2, x_3) and we consider wave directions only in (x_2, x_3). Similarly, we could reverse the roles of x_1 and x_2 here.

5.2 Controlled Illumination at Depth in a Heterogeneous Medium

We consider here the controlled illumination problem of Rietveld's [1995] and Rietveld et al [1992]. To this end, we introduce

$$u_{\mathrm{H}}(\boldsymbol{x}_H, \omega) \equiv 1, \quad \boldsymbol{x}_H = (x_1, x_2, H). \tag{61}$$

As a first step, we need to *back-project* this wave to the acquisition surface where we have the observed data. To derive that result, we can extrapolate from the propagation processes of Section 3.2 where we derived the wave field representation for a wave given on a boundary surface. In particular, we would apply Green's theorem to a hemispherical region, now with the cap on the bottom and the hemispherical half-space above. In this case, the wave field is *incoming* in this domain and we must therefore use an incoming Green's function in order to apply Green's theorem. This will lead to a wave field representation similar to the first line of equation (42) for u_{D} with the following changes:

(i) We integrate over the surface, $x_3' = H$;
(ii) We use $\overline{G_{\mathrm{D}}}$ as the incoming wave;
(iii) $\partial/\partial n' = \partial/\partial x_3'$ on the surface where $x_3' = H$.

This all leads to the following representation for $u_{\mathrm{H}}(\boldsymbol{x}, \omega)$.

$$u_{\mathrm{H}}(\boldsymbol{x}, \omega) = 2i\omega \int_{x_3'=H} \frac{\overline{G_{\mathrm{D}}(\boldsymbol{x}, \boldsymbol{x}', \omega)}}{\mathrm{v}(\boldsymbol{x}_H')} dx_1' dx_2', \tag{62}$$

$x_3 < H$.

Here, since the phase is constant on the plane,

$$\boldsymbol{p}(\boldsymbol{x}_H') = (0, 0, 1/\mathrm{v}(\boldsymbol{x}_H'));$$

we have used the last element here for p_3 required in the forumula of equation (42) in order to produce the representation of u_H in equation (62). By writing this function in such general terms, we include all caustic effects, including multiple arrivals and phase shifts that might occur in the back projection simply by using a sufficiently accurate Green's function. Of course, this representation could as easily be replaced by solving the one-way or two-way wave equation for u_{H} to determine its values at the upper surface. When we use the WKBJ approximation of the Green's function, we have to take care to include all of the multiple arrivals and phase shifts in that representation.

We can now use the synthesis method described in Section 3.2. In particular, we use $u_{\mathrm{H}}(\boldsymbol{x}, \omega)$ for the function $u(\boldsymbol{x}, \omega)$ in equations (41) and (42). We have no need to compute $u_{\mathrm{D}}(\boldsymbol{x}, \omega)$ at depth–the first line in equation (42)–since we would not use this solution at arbitrary depth, but only at $x_3 = H$; there the down going wave is just the unidirectional wave of unit amplitude given by equation (61). However, we can use $u_{\mathrm{H}}(\boldsymbol{x}, \omega)$ to compute $u_{\mathrm{R}}(\boldsymbol{x}, \omega)$ by using the second equation in (42). That is,

$$u_{\mathrm{R}}(\boldsymbol{x}_r, \omega) = -2 \int_{x_3'=0} G_{\mathrm{R}}(\boldsymbol{x}_r, \boldsymbol{x}', \omega) \cdot \frac{\partial u_{\mathrm{H}}(\boldsymbol{x}', \omega)}{\partial x_3'} dx_1'' dx_2''. \tag{63}$$

Recall that $G_{\mathrm{R}}(\boldsymbol{x}_r, \boldsymbol{x}', \omega)$ is the observed point source response data and $u_{\mathrm{R}}(\boldsymbol{x}_r, \boldsymbol{x}', \omega)$ is the synthesized data that would be the response to $u_{\mathrm{H}}(\boldsymbol{x}', \omega)$ evaluated at $x_3' = 0$.

5.2.1 Downward continuation of the synthesized data and inversion

Now we can downward continue the data $u_{\mathrm{R}}(\boldsymbol{x}_r, \omega)$ into the Earth by using equation (46). That is,

$$u_{\mathrm{R}}(\boldsymbol{x}, \omega) = -4 \int_{x_{r3}=0} dx_{r1} dx_{r2} \frac{\partial \overline{G_{\mathrm{D}}(\boldsymbol{x}, \boldsymbol{x}_r, \omega)}}{\partial x_{r3}} \cdot \int_{x_3'=0} dx_1' dx_2' G_{\mathrm{R}}(\boldsymbol{x}_r, \boldsymbol{x}', \omega) \cdot \frac{\partial u_{\mathrm{H}}(\boldsymbol{x}', \omega)}{\partial x_3'}. \tag{64}$$

Next, we use the imaging condition of equation (54) for imaging and inversion. However, it only makes sense to use this at the depth $x_3 = H$ where the downward propagating synthesizing wave is identically equal to one; see equation (61). That is, we write

$$\begin{aligned} \mathcal{R}(\boldsymbol{x}_H, \theta) \quad = \quad & -\frac{2}{\pi} \int d\omega \int_{x_{r3}=0} dx_{r1} dx_{r2} \\ & \cdot \frac{\partial \overline{G_{\mathrm{D}}(\boldsymbol{x}, \boldsymbol{x}_r, \omega)}}{\partial x_{r3}} \\ & \cdot \int_{x_3''=0} dx_1' dx_2' G_{\mathrm{R}}(\boldsymbol{x}_r, \boldsymbol{x}', \omega) \\ & \cdot \frac{\partial u_{\mathrm{H}}(\boldsymbol{x}', \omega)}{\partial x_3'}, \\ & \boldsymbol{x}_H = (x_1, x_2, H). \end{aligned} \tag{65}$$

Let us review the steps of this inversion.

(i) Extrapolate the plane wave at depth $x_3 = H$ to the upper surface, $x_3 = 0$.

(ii) Use this wave field at $x_3 = 0$ to synthesize the reflection response to the unit amplitude illuminating wave at depth $x_3 = H$.

(iii) Downward continue the synthesized data to the depth $x_3 = H$.

(iv) Compute the reflectivity function by the standard imaging condition, an integral over ω.

When we compare this synthesis/inversion with the more standard case, where the boundary data is given at $x_3 = 0$, there is only one difference in the procedures. The first step here would be replaced by a downward propagation of the data $u_{\rm D}$ prescribed at the upper surface. This is an equivalent computation. However, here, at the imaging depth, we know the incidence wave with which the process was started, so that step is not necessary.

5.3 Synthesis and Inversion for a Unidirectional wave in a depth-dependent medium or a homogeneous medium

Let us now suppose that the wave speed depends at most on the depth x_3: $\mathrm{v} \equiv \mathrm{v}(x_3)$. Then, in place of the unit wave of equation (61), we introduce the following.

$$u_{\rm H}(\boldsymbol{x}_{H},\omega) = \exp\{i\omega \boldsymbol{p}_{H}\cdot \boldsymbol{x}_{H}\}, \quad \boldsymbol{p}_{H} = \frac{\hat{\boldsymbol{p}}_{H}}{\mathrm{v}(H)}, \tag{66}$$

with $\hat{\boldsymbol{p}}_{H}$ a constant unit vector. This wave is unidirectional at the depth H, but not restricted to vertical incidence. The back-projected wave in the upward direction is represented as only a minor modification of the previous upward projected wave of equation (62); that is,

$$u_{\rm H}(\boldsymbol{x},\omega) = 2i\omega\frac{\hat{p}_{H3}}{\mathrm{v}(H)}\int_{x_3'=H}\exp\{i\omega\boldsymbol{p}_{H}\cdot\boldsymbol{x}_{H}\} \cdot\overline{G_{\rm D}(\boldsymbol{x},\boldsymbol{x}',\omega)}dx_1'dx_2', \tag{67}$$

$$x_3 < H.$$

Given this representation of the back-projected wave field at $x_3 = 0$, the representation of equation (63) for the synthesized reflection response remains the same, as does the downward continuation of these synthesized data given by equation (64). We do need to modify the inversion formula of equation (65), since the incident wave at depth H was identically one in the previous case, while here it is given by equation (66). We find that the reflectivity is now given by

$$\begin{aligned}\mathcal{R}(\boldsymbol{x}_{H},\theta) &= -\frac{2}{\pi}\int d\omega\exp\{-i\omega\boldsymbol{p}_{H}\cdot\boldsymbol{x}_{H}\} \\ &\quad\cdot\int_{x_{r3}=0}dx_{r1}dx_{r2}\frac{\partial\overline{G_{\rm D}(\boldsymbol{x},\boldsymbol{x}_r,\omega)}}{\partial x_{r3}} \\ &\quad\cdot\int_{x_3''=0}dx_1'dx_2'G_{\rm R}(\boldsymbol{x}_r,\boldsymbol{x}',\omega) \\ &\quad\cdot\frac{\partial u_{\rm H}(\boldsymbol{x}',\omega)}{\partial x_3'}.\end{aligned} \tag{68}$$

Note that the formulas presented in this section remain unchanged when the wave speed is constant, that is, in a homogeneous medium. Only the specific Green's functions in these formulas change.

We have now presented inversion formulas for synthesized common-source data sets. The synthesis uses incident waves at the upper surface or at depth and extended sources. The various steps before imaging and inversion are represented here by Kirchhoff integrals that propagate data on a given plane back into the Earth or up to the acquisition surface. Those propagations could be carried out for any accuracy of asymptotic approximate Green's function or by solving the appropriate (one-way) wave equation.

6 COMMUTING SYNTHESIS AND INVERSION

As noted in the introduction, synthesis is a mechanism that allows us to process data over the entire range of a seismic survey rather than over the range of the individual shots. Furthermore, the wavefields we create through synthesis are solutions of a single wave equation, in contrast to common-offset data, which is not. Despite the clear advantages of synthesis, here we examine the possibility of postponing synthesis, carrying out inversion first, despite the seeming inefficiency of this commutation of operations.

It should be noted that synthesis typically provides an image and parameter estimation capability for only one incidence direction at each image point. It is necessary therefore to carry out a suite of synthesis operations in order to obtain the most complete inversion available from the data, that is, with all of the varying incidence directions available from the data at each image point.

If there were an advantage to synthesizing before inverting, it would arise from the "count" of necessary syntheses versus the count of necessary common-shot inversions to extract the same information from a survey. On the other hand, there is flexibility gained by postponing synthesis until after the modeling step. For example, a few common-shot inversions might indicate dominant dips in the neighborhood of a target. Then, synthesis of only a few plane waves of varying dip—at the upper surface or in the target region—might lead to making the "count" in this order significantly less than in the process that starts from synthesizing first.

Inverting synthesized data consists of three steps:

(i) synthesize the source wave and the observed wave at the acquisition surface;

(ii) downward propagate both of the synthesized wave fields;

(iii) form the frequency dependent impedance quotient from the downward propagated waves at each image point and integrate over frequency to obtain the reflectivity function.

Steps 1 and 2 can be interchanged to produce the alternative we propose here. This works because modeling and synthesis are integration techniques that commute. This is literally true for Kirchhoff modeling, but it is also true for ray theoretic modeling (including Gaussian beam modeling) or WEM. The latter modeling techniques are equivalent to convolution-type integration of data with an exact Green's function followed by various levels of asymptotic analysis. In what follows in this section, we show in some detail how this reversal of order works for the Kirchhoff approach to synthesis and inversion.

6.1 Analysis

The fundamental inversion equation for synthesized data is equation (55). Let us separate off the frequency integral here and consider only the spatial integral. This is a frequency dependent reflectivity or impedance for each choice of ω; that is,

$$\begin{aligned}\mathcal{R}_\omega(\boldsymbol{x},\theta,\omega) &= \frac{1}{u_{\mathrm{D}}(\boldsymbol{x},\omega)} \int_{x_{r3}=0} u_{\mathrm{R}}(\boldsymbol{x}_r,\omega) \\ &\qquad \cdot \frac{\partial \overline{G_{\mathrm{D}}(\boldsymbol{x},\boldsymbol{x}_r,\omega)}}{\partial x_{r3}} dx_{r1}dx_{r2} \\ &= \frac{u_{\mathrm{R}}(\boldsymbol{x},\omega)}{2u_{\mathrm{D}}(\boldsymbol{x},\omega)} \end{aligned} \tag{69}$$

$$\begin{aligned}\mathcal{R}(\boldsymbol{x},\theta) &= \frac{1}{\pi}\int \mathcal{R}_\omega(\boldsymbol{x},\theta,\omega)d\omega \\ &= \frac{1}{2\pi}\int \frac{u_{\mathrm{R}}(\boldsymbol{x},\omega)}{u_{\mathrm{D}}(\boldsymbol{x},\omega)}d\omega.\end{aligned}$$

Here, in the first line, $u_{\mathrm{D}}(\boldsymbol{x},\omega)$ can be moved outside the integration because it is independent of the receiver variables over which that integration is carried out. Then, the integration in the first line of this equation is simply half of the modeling operator of equation (46). This accounts for the second equality for $\mathcal{R}_\omega$ in the first equation. The second equation simply reminds us of the relationship between $\mathcal{R}_\omega(\boldsymbol{x},\theta,\omega)$ and $\mathcal{R}(\boldsymbol{x},\theta)$ of equation (54). Below, we refer to R_ω as an impedance.

It is necessary at this point to discuss waves synthesized by a prescribed source at the acquisition surface from waves synthesized by a prescribed incident wave at the acquisition surface.

6.2 Synthesis via a prescribed source

When the wave is synthesized by a source on the acquisition surface, we called that source function $f(\boldsymbol{x},\omega)$ and then equation (17) gives the synthesized downward propagation of the function $u_{\mathrm{D}}(\boldsymbol{x},\omega)$ and the synthesized response. In the expression for u_R in that equation, we restrict the argument of u_{R} to $\boldsymbol{x}_r$ because this is the only place that we have the observed data $G_{\mathrm{R}}(\boldsymbol{x}_r,\boldsymbol{x}',\omega)$, as we have noted earlier.

Let us restrict the source mechanism to the acquisition surface and write

$$f(\boldsymbol{x}',\omega) = \delta(x_3')f_s(x_1',x_2',\omega), \tag{70}$$

so that $u_{\mathrm{D}}(\boldsymbol{x},\omega)$ in equation (17) becomes

$$u_{\mathrm{D}}(\boldsymbol{x},\omega) = \int_{x_3'=0} f_s(x_1',x_2',\omega)G_{\mathrm{D}}(\boldsymbol{x},\boldsymbol{x}'\omega)dx_1'dx_2'. \tag{71}$$

We can see here that this is just a Green's function representation of $u_{\mathrm{D}}(\boldsymbol{x},\omega)$ at depth derived from the downward component of the point source wavefields used in the original seismic experiments.

Similarly,

$$\begin{aligned}u_{\mathrm{R}}(\boldsymbol{x}_r,\omega) = \int_{x_3'=0} & f_s(x_1',x_2',\omega) \\ & \cdot G_{\mathrm{R}}(\boldsymbol{x}_r,\boldsymbol{x}',\omega)dx_1'dx_2'.\end{aligned} \tag{72}$$

Then, equation (46) tells us how to downward propagate these data to determine u_{R} at depth. We then substitute into equation (69) to obtain an expression for the impedance R_ω. That is

$$\begin{aligned}\mathcal{R}_\omega(\boldsymbol{x},\theta,\omega) = \frac{1}{u_{\mathrm{D}}(\boldsymbol{x},\omega)} \int_{x_{r3}=0}\int_{x_3'=0} & f_s(x_1',x_2',\omega) \\ & \cdot G_{\mathrm{R}}(\boldsymbol{x}_r,x_1',x_2',0,\omega) \\ & \cdot \frac{\partial \overline{G_{\mathrm{D}}(\boldsymbol{x},\boldsymbol{x}_r,\omega)}}{\partial x_{r3}} \\ & \cdot dx_{r1}dx_{r2}dx_1'dx_2'.\end{aligned} \tag{73}$$

In this equation, the integration over (x_{r1},x_{r2}) is just the downward projection of the observed data $G_{\mathrm{R}}(\boldsymbol{x}_r,x_1',x_2',0,\omega)$ from the individual shot located at $(x_1',x_2',0)$. The integration over $(x_1',x_2',0)$ then provides the downward projection of the synthesized observations at the acquisition surface. Thus,

$$\begin{aligned}G_{\mathrm{R}}(\boldsymbol{x},x_1',x_2',0,\omega) = \int_{x_{r3}=0} & G_{\mathrm{R}}(\boldsymbol{x}_r,x_1',x_2',0,\omega) \\ & \cdot \frac{\partial \overline{G_{\mathrm{D}}(\boldsymbol{x},\boldsymbol{x}_r,\omega)}}{\partial x_{r3}} dx_{r1}dx_{r2}\end{aligned} \tag{74}$$

propagates the point source response at the acquisition

surface back into the Earth. If we use this representation of $G_{\rm R}$ at depth in equation (73) for $\mathcal{R}_\omega$ we find that

$$\mathcal{R}_\omega(\boldsymbol{x},\theta,\omega) = \frac{1}{u_{\rm D}(\boldsymbol{x},\omega)} \int\limits_{x_{r3}=0} \int\limits_{x_3'=0} f_s(x_1',x_2',\omega) \cdot G_{\rm R}(\boldsymbol{x},x_1',x_2',0,\omega)dx_1'dx_2' \quad (75)$$
$$= \frac{u_{\rm R}(\boldsymbol{x},\omega)}{2u_{\rm D}(\boldsymbol{x},\omega)}.$$

This representation of $\mathcal{R}_\omega$ should be compared to the definition of $\mathcal{R}_\omega$ in equation (69). There, we downward propagated the wave synthesized from point source responses into the Earth; here, we synthesized the same wave at depth by downward propagating the point source data sets and then synthesizing. This is the commutation of operators that we claimed, leading to the same function, $\mathcal{R}_\omega$.

After computing $G_{\rm R}$ as in equation (74) for each shot $(x_1', x_2', 0)$ and each ω, we have options available for further processing. First, division by the downward propagated point source from $(x_1', x_2', 0)$, namely, $G_{\rm D}(\boldsymbol{x},\boldsymbol{x}',\omega)$, and integration over ω yields common-shot inversion for each shot:

$$\mathcal{R}(\boldsymbol{x},\boldsymbol{x}_s,\theta) = \frac{1}{2\pi}\int \frac{G_{\rm R}(\boldsymbol{x},\boldsymbol{x}_s,\omega)}{G_{\rm D}(\boldsymbol{x},\boldsymbol{x}_s,\omega)}d\omega. \quad (76)$$

Here, we have replaced the variable $\boldsymbol{x}'$ by the variable $\boldsymbol{x}_s$ and added this argument to $\mathcal{R}$ to emphasize that this is a reflectivity function for each shot. This is equivalent to using the source function $f(\boldsymbol{x}',\omega) = \delta(x_3')f_s(x_1',x_2',\omega) = \delta(x_3')\delta(x_1'-x_{s1})\delta(x_2'-x_{s2})$. We have neglected a source signature for this discussion.

A second option is to carry out the synthesis to generate the impedance function $\mathcal{R}_\omega$ of equation (75), namely, integration over (x_1', x_2'), to complete the frequency dependent impedance function of that equation. Then, integration over ω produces the inversion of the wave field for the synthesized source, $\delta(x_3')f_s(x_1',x_2',\omega)$. In this case, we obtain the second representation of $\mathcal{R}$ of equation (69).

6.3 Synthesis via a prescribed incident wave

When an incident wave is prescribed on the acquisition surface, we use the synthesized wavefield representations in equation (42) for the downward propagating incident wave and the synthesized response at the upper surface. Those representations should be compared to the synthesis formulas of equations (71) and (72). We see that the only difference is that the source function in the integrals of those equations is replaced here by the vertical (normal) derivative of the prescribed wave field.

Thus, the frequency dependent impedance function of equation (73) is now replaced by

$$\mathcal{R}_\omega(\boldsymbol{x},\theta,\omega) = \frac{1}{u_{\rm D}(\boldsymbol{x},\omega)} \int\limits_{x_{r3}=0} \int\limits_{x_3'=0} \frac{\partial u(\boldsymbol{x}',\omega)}{\partial x_3'} \cdot G_{\rm R}(\boldsymbol{x}_r,x_1',x_2',0,\omega) \cdot \frac{\partial \overline{G_{\rm D}(\boldsymbol{x},\boldsymbol{x}_r,\omega)}}{\partial x_{r3}} \cdot dx_{r1}dx_{r2}dx_1'dx_2'. \quad (77)$$

As in the previous discussion, the integration over (x_{r1}, x_{r2}) is merely the downward propagation of the observed common-shot response data at the upper surface and its representation is exactly as in equation (74) and produces the same output, namely, $G_{\rm R}(\boldsymbol{x},x_1',x_2',0,\omega)$. Carrying out this integration for each source position (x_1', x_2') amounts to modeling before synthesis. As noted above, this modeling step could be carried out by alternative modeling procedures. We now obtain an alternative representation of the frequency dependent impedance R_ω with commuted modeling and synthesis as in equation (75):

$$\mathcal{R}_\omega(\boldsymbol{x},\theta,\omega) = \frac{1}{u_{\rm D}(\boldsymbol{x},\omega)} \int\limits_{x_{r3}=0} \int\limits_{x_3'=0} \frac{\partial u(\boldsymbol{x}',\omega)}{\partial x_3'} \cdot G_{\rm R}(\boldsymbol{x},x_1',x_2',0,\omega)dx_1'dx_2' \quad (78)$$
$$= \frac{u_{\rm R}(\boldsymbol{x},\omega)}{2u_{\rm D}(\boldsymbol{x},\omega)}.$$

Now, the reflectivity function $\mathcal{R}(\boldsymbol{x},\theta)$ is again calculated by using the second representation of (69).

6.4 Commuting

We have now presented formulas for generating inversion formulas for synthesized waves, by synthesizing over the ensemble of common-shot inversions. We did this for both synthesized sources and for synthesized incident waves. The utility of these results is unclear at this point, but the results are presented for consideration.

7 SUMMARY AND CONCLUSIONS

We have described a general theory of synthesis of sources or incident waves and their reflection responses from an ensemble of common-shot data records. The theory is close to the method expounded in Wapenaar et al [1989] with one application, controlled illumination, being the method of Rietveld et al [1992] and Rietveld [1995]. The method here is based on careful application of Green's theorem for waves generated by boundary

data or waves generated by sources. On the other hand, synthesis starting from a unidirectional wave at depth, with appropriate constraint on the wavespeed, has not been previously presented.

We assumed that all datum surfaces are planar. That allowed us to obtain Green's functions for which either the function or its normal derivative is zero on the datum surface in terms of the Green's functions of common-shot data gathers. Thus, we can fit the solution representation to the only data we have—the observations of the reflected common-shot data—and lacking the normal derivative of that data. We further presented a theory for computing the response to synthesized sources or synthesized incident waves from the ensemble of common-shot inversions.

Our results are expressed in terms of general Green's functions, leaving to the user the option of how accurate a Green's function will be used in the implementation. We expect that the hierarchy of progressively more accurate Green's functions will provide higher quality images. However, in all cases, the output of the inversion will be an angularly dependent reflection coefficient scaled by the area under the source signature whenever the multiple speculars at the image point can be separated.

ACKNOWLEDGEMENTS

Yu Zhang proposed this topic and Sam Gray provided guidance to the related literature. I am grateful to both of them for the roles they played in bringing this project to fruition.

REFERENCES

Bleistein, N., 1984, Mathematical Methods for Wave Phenomena: Academic Press, New York.

Bleistein, N., Y. Zhang, and G. Zhang, S. H. Gray, 2005, Migration/inversion: think image point coordinates, process in acquisition surface coordinates: Inverse Problems 21, 1715-1744.

Erdélyi, A., Magnus, W., M. Oberhettinger, F., Tricomi, F. G., 1953, Higher Transcendental Functions, Vol. II: McGraw-Hill, New York.

Hanitzsch, C., 1997, Comparision of weights in prestack amplitude-preserving Kirchhoff depth migration: Geophysics, 62, 1812-1816.

Keho, T. H. and W. B. Beydoun, 1988, Paraxial ray Kirchhoff migration: Geophysics, **53**, 12, 1540-1546.

Reitveld, W. E. A., 1995, Controlled Illumination in Prestack Seismic Migration: Ph. D. Thesis, Delft Technical University, Delft.

eitveld, W. E. A., A. J. Berkhout and C. P. A. Wapenaar, 1992, Optimum seismic illumination of hydrocarbon reservoirs: Geophysics, 57, 10, 1334-1345.

Wapenaar, C. P. A., G. L. Peels, V. Budejicky, A. J. Berkhout, 1989, Inverse extrapolation of primary seismic waves: Geophysics, 54, 7, 853-863.

Xie, X-B, J. Shengwen and R-S Wu, 2004, Wave equation based illumination analysis: SEG Expanded Abstracts, 23 (Denver), 933-936, Tulsa.

Zhang, W., 2004, 3D depth migration with plane wave synthesizing method: SEG Expanded Abstracts 23 (Denver), 1073-1076, Tulsa.

Zhang, Y, G. Zhang and N. Bleistein, 2003, True Amplitude Wave Equation Migration Arising from True Amplitude One-way Wave Equations: Inverse Problems, **19**, 5, 1113-1138.

Zhang, Y., Sun, J., C. Notfors, S. H. Gray, L. Chernis, and J. Young, 2005., Delayed-shot 3D depth migration: Geophysics, 70, 5, E21-E28.